Journal of Inclusion Phenomena and Macrocyclic Chemistry (2006) 56: 69–74
DOI 10.1007/s10847-006-9063-8

Characterization of an Inclusion Complex of 5,10,15,20-Tetrakis(4-sulfonatophenyl)-porphinato Iron and an *O*-Methylated *β*-Cyclodextrin Dimer Having a Pyridine Linker and Its Related Complexes in Aqueous Solution

KOJI KANO*, HIROAKI KITAGISHI and SHIGEKI TANAKA
Department of Molecular Science and Technology, Doshisha University, Kyotanabe 610-0321, Kyoto, Japan

Key words: characterization, ESI-MS, MM calculation, myoglobin model, NMR, *O*-methylated *β*-cyclodextrin dimer, tetrakis(4-sulfonatophenyl)porphinato iron

Abstract

The structure of a carbon monoxide adduct (CO-hemoCD) of a 1:1 complex of 5,10,15,20-tetrakis(4-sulfonatophenyl)porphinato iron(II) (Fe(II)TPPS) and an *O*-methylated *β*-cyclodextrin dimer having a pyridine linker (**1**) has been determined by means of NMR spectroscopy and molecular mechanics (MM) calculation. The results indicate the structure as that the sulfonatophenyl groups at the 5- and 15-positions of Fe(II)TPPS are incorporated into two cyclodextrin cavities of **1** to form a 1:1 inclusion complex (hemoCD), whose Fe(II) center is coordinated by a carbon monoxide (CO) molecule. CO-hemoCD possesses a C_{2v} symmetrical nature that is supported by MM calculation. The energy minimized structure of CO-hemoCD suggests that the CO–Fe(II) part is significantly covered by two cyclodextrin moieties resulting in a cage effect in CO binding phenomenon. Other spectroscopic results of relating complexes also support the structure of hemoCD deduced from the results concerning CO-hemoCD.

Introduction

One of the important subjects in biomimetic chemistry is modeling functions of biological systems in aqueous media. However, modeling of biological functions is strictly restricted because of limitation of available compounds that are soluble in water. Water-soluble porphyrins are widely usable compounds because there are many important metal proteins having metal porphyrins as prosthetic groups. Meanwhile, cyclodextrins (CDs) have been utilized as simple enzyme models due to their ability to include various hydrophobic molecules and ions through weak intermolecular interactions [1]. CDs have been regarded as hydrophobic pockets of enzymes. Several years ago, we started to use CDs as simple protein models that prepare metal protein mimics.

Several research groups have studied interactions of water-soluble porphyrins and CDs. Hirai et al. reported complexation of deuteroporphyrin IX, hematoporphyrin IX, and coproporphyrin III without aryl groups at the meso-positions of the porphyrins with *γ*-CD [2]. Since there is no part in these porphyrins that is included by *γ*-CD, the binding constants (*K*) for complexation are very small (16–35 M^{-1}). Some synthetic porphyrins having ionic aryl substituents at the meso-positions have been shown to form relatively stable complexes of CDs and the porphyrins. Inclusion of ionic aryl substituents of a porphyrin by CD was first reported by Manka and Lawrence who found the formation of a *trans*-type 2:1 complex of heptakis(2,6-di-*O*-methyl)-*β*-CD (2,6-DMe-*β*-CD) and an cationic porphyrin [3]. The result suggests a strong ability of 2,6-DMe-*β*-CD to include an aryl group at the meso-position of a tetra-arylporphyrin. Mosseri et al. studied complexation of anionic metalloporphyrins such as Fe(III)TPPS and Zn(II)TPPS (TPPS: 5,10,15,20-tetrakis(4-sulfonatophenyl)porphyrin) with *β*-CD [4]. On the basis of ^{1}H NMR data, Ribó et al. assumed the formation of a *trans*-type 2:1 complex of *β*-CD and TPPS [5]. Other research groups, however, reported the *K* values for complexation of TPPS with *β*-CD (440–5600 M^{-1}) by assuming a 1:1 complex [6].

We previously found that two heptakis(2,3,6-tri-*O*-methyl)-*β*-CD (TMe-*β*-CD) molecules strongly include the peripheral substituents at the 5- and 15-positions of TPPS in aqueous solution [7]. The *K* value of this system is too large to be determined. The pK_a value for protonation to the pyrrole nitrogen atoms is ca. 4.8 in water without CD [8] while it is reduced to 0.4 in the presence of TMe-*β*-CD [7a], indicating that a porphyrin center is placed at a very hydrophobic cleft formed by two TMe-*β*-CD molecules. Such a nature of per-*O*-methylated *β*-CD was utilized to mimic the function of met-myoglobin (metMb) that selectively binds inorganic anions to its Fe(III) center [9]. Further extension of this study realized

* Author for Correspondence. E-mail: kkano@mail.doshisha.ac.jp

modeling the function of myoglobin (Mb) [10]. We prepared an *O*-methylated β-cyclodextrin dimer (**1**) as shown in Figure 1 as a globin model. The dimer **1** forms an extremely stable 1:1 complex of Fe(II)TPPS that reversibly binds dioxygen (O_2) [10]. Determination of the structures of the 1:1 complexes of Fe(III)TPPS and Fe(II)TPPS with the dimer **1** in aqueous solution is difficult because of the paramagnetic nature of these iron complexes. In such a cased, the structure of the complex should be deduced from many experimental data that suggest a single structure. In the present study, we characterized the complex of FeTPPS and **1** by means of UV–vis, ESI-MS, and NMR spectroscopy. The abbreviations used in this paper are shown in Figure 1.

Results and discussion

Characterization of Fe(III)TPPS and Zn(II)TPPS complexes with the dimer **1**

As shown in the previous communication [10], the absorption spectrum of Fe(III)TPPS in phosphate buffer at pH 5.0 systematically changes upon addition of the dimer **1**, and the spectral change levels off after the addition of one-equivalent of **1**, indicating the formation of a very stable 1:1 complex of Fe(III)TPPS and **1**. The pH value of 5 was chosen to minimize the formation of a μ-oxo dimer of Fe(III)TPPS. The formation of the 1:1 complex of Fe(III)TPPS and the dimer **1** was definitely confirmed by means of ESI-MS spectroscopy (Figure 2). The spectrum was measured for a sample of a 1:1 mixture of Fe(III)TPPS and the dimer **1** in water (pH 4.5) using a negative mode. A main peak was observed at m/z 1307 that is corresponding to $[Fe(III)TPPS\text{-}\mathbf{1}]^{3-}$ (mol wt 3923). Another peak was detected at m/z 985 that is ascribed to $[Fe(III)(OH)TPPS\text{-}\mathbf{1}]^{4-}$ (mol wt 3940). On the basis of these results, it is reasonable to assume the formation of met-hemoCD whose structure is shown in Figure 1.

Although the μ-oxo dimer was formed in aqueous solution in the pH region between 5 and 8, it was converted to the 1:1 complex of Fe(III)TPPS and **1** upon addition of the dimer **1**. The UV–vis spectral changes of a mixture of Fe(III)TPPS and **1** as a function of pH are shown in Figure 3. In the pH range between 9.88 and 2.83, the systematic spectral changes with two isosbestic points were observed, indicating a single ligand exchange of the Fe(III)TPPS-**1** complex. At pH < 2, another type of the spectral change was measured. Plausible pD-dependent equilibria of the Fe(III)TPPS-**1** complex are shown in Figure 3. In order to figure the structure at each pH range, paramagnetic ^{1}H NMR spectra of the Fe(III)TPPS-**1** complex were measured in D_2O at various pDs. The results are shown in Figure 4. At pH 8.7, the signal due to the pyrrole β-protons was observed at 84 ppm as a broad singlet, suggesting the formation of a complex in a 5-coordinate high spin state [11]. The corresponding species is OH^- coordinated met-hemoCD where the proximal pyridine of **1** does not bind to the Fe(III) center. At pD 4.4, the pyrrole β-protons were observed at 51, 53, and 55 ppm. The high-field shifts upon lowering pD suggest conversion of monohydroxo complex of met-hemoCD to the pyridine-coordinated met-hemoCD in an admixed intermediate

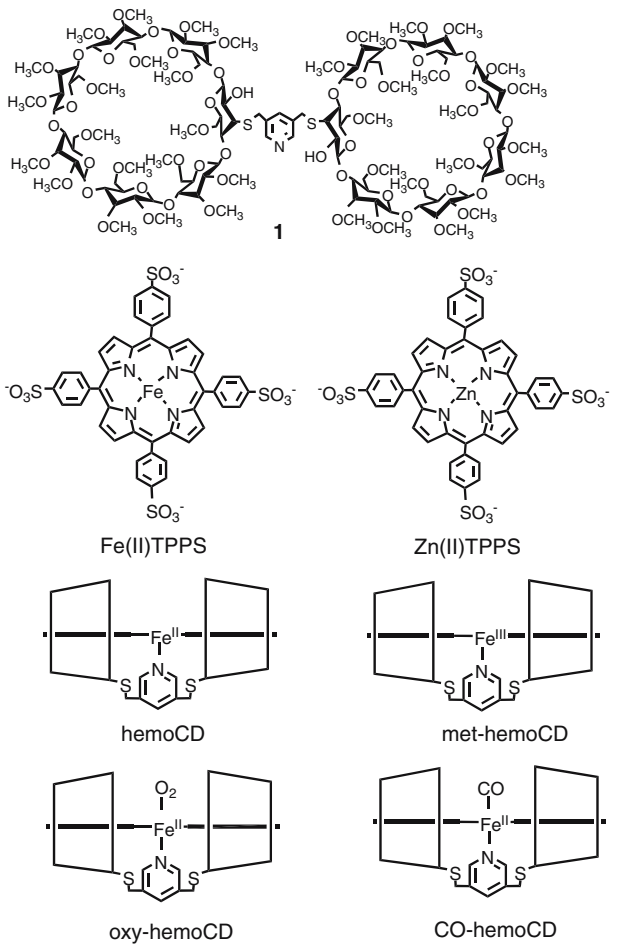

Figure 1. Structures of the host (**1**) and the guests used in this study and the abbreviations of the inclusion complexes.

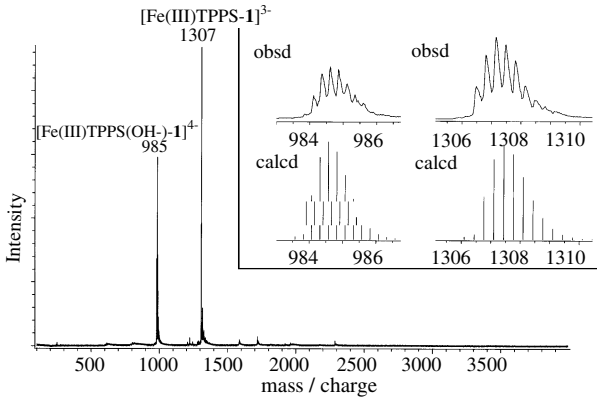

Figure 2. ESI-MS spectrum (negative mode) of the Fe(III)TPPS-**1** complex (met-hemoCD, molecular weight = 3923) in water at pH 4.5. The concentration of met-hemoCD was 5×10^{-4} M. The theoretical isotope peaks of both fragments are in good agreement with those of the assumed structures.

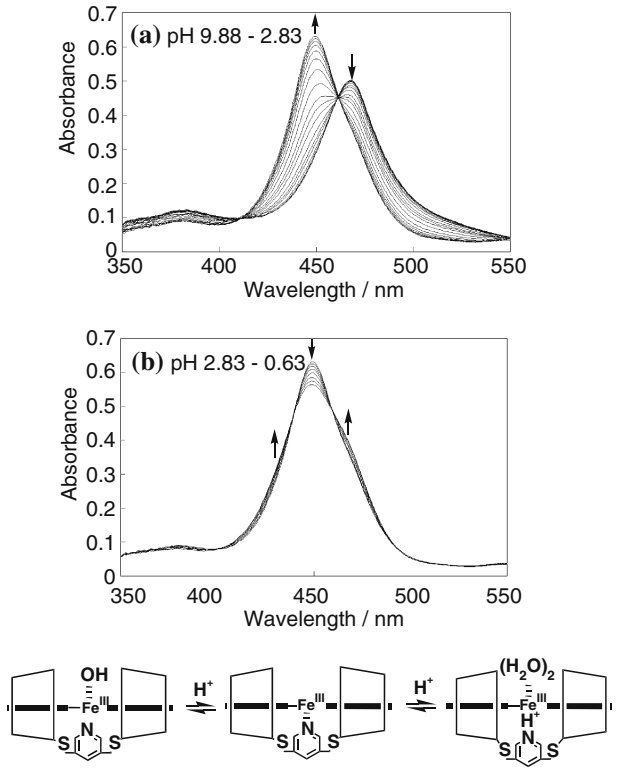

Figure 3. UV–vis absorption spectral changes of Fe(III)TPPS (5×10^{-6} M) complexed with **1** (6×10^{-6} M) as a function of pH in aqueous 0.1 M $NaClO_4$ solution at 25 °C. The pH values were adjusted by NaOH and $HClO_4$.

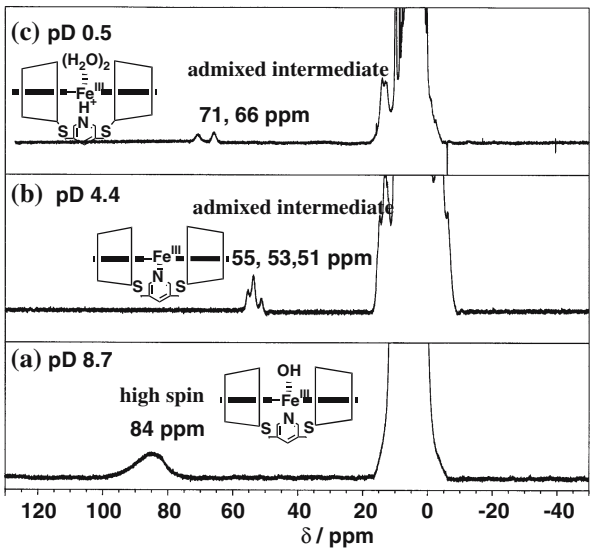

Figure 4. ^{1}H NMR spectra of Fe(III)TPPS/**1** complex at various pHs: [Fe(III)TPPS] = 3 mM, [**1**] = 3 mM. The pDs were adjusted by $HClO_4$ and NaOD in D_2O containing 0.1 M $NaClO_4$.

spin state [11]. The irregular NMR signals due to the pyrrole β-protons suggest a disturbance in symmetry of met-hemoCD due to coordination of the pyridine moiety to the Fe(III) center. If the pyridine-coordinated met-hemoCD has a C_{2v} symmetry, two-types of the signals should be detected. In acidic D_2O at pD 0.5, two singlet signals due to the pyrrole β-protons of met-hemoCD having a C_{2v} symmetrical nature were measured at 66 and 71 ppm, which are ascribed to the signals due to diaqua complex of met-hemoCD in an admixed intermediate spin state [12] where a pyridine nitrogen is protonated leading to dissociation of the pyridine-Fe(III) coordination bond.

It is assumed that inclusion phenomenon of Fe(III)TPPS differs from that of Fe(II)TPPS because one positive net charge remains at a porphyrin center of Fe(III)TPPS while the net charge of Fe(II)TPPS is zero [9]. In place of a relatively labile Fe(II)TPPS, we used Zn(II)TPPS to deduce the characteristics of the complex of Fe(II)TPPS and the dimer **1** (hemoCD). Figure 5 shows the UV–vis spectral changes of Zn(II)TPPS in phosphate buffer at pH 8.0 upon addition of the dimer **1**. These systematic changes mean the formation of a single product. The spectral titration curve clearly indicate the 1:1 complex of Zn(II)TPPS and **1**. Since the absorption maximum of the 1:2 inclusion complex of Zn(II)TPPS and monomeric TMe-β-CD was observed at 424 nm and the new absorption band appeared at 429 nm is corresponding to an absorption maximum of pyridine-coordinated Zn(II)TPPS reported by Nappa and Valentein [13], the most plausible structure of the 1:1 complex of Zn(II)TPPS and the dimer **1** is figured as that two sulfonatophenyl groups at the 5- and 15-positions of Zn(II)TPPS are incorporated into two *O*-methylated β-CD cavities of **1**, where the Zn(II) center is coordinated by the proximal pyridine of the dimer **1**. The pH-dependent spectral changes of the Zn(II)TPPS-**1** complex is shown in Figure 6. Unlike with the case of the Fe(III)TPPS-**1** complex, a single spectral change was observed. A monotonous decrease in the absorbance at 429 nm at pH below 3 is ascribed to the dissociation of the Zn(II)-pyridine coordination bond due to the protonation to a pyridine nitrogen. Since the pK_a value of pyridine is 5.4, the protonation to the pyridine itself nitrogen of the dimer **1** is significantly inhibited by the complexation with Zn(II)TPPS.

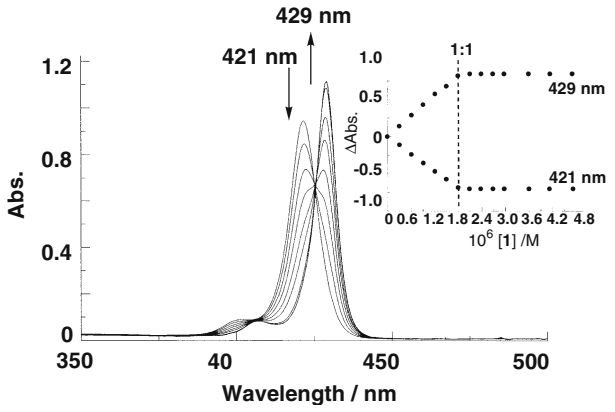

Figure 5. UV–vis absorption spectral changes of Zn(II)TPPS (1.8×10^{-6} M) as a function of [1] in 0.1 M phosphate buffer at pH 8.0 and 25 °C.

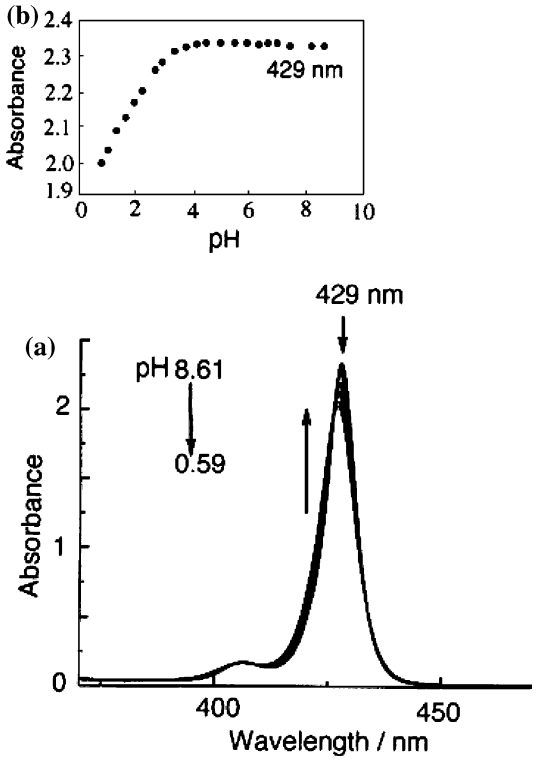

Figure 6. UV–vis absorption spectral changes of Zn(II)TPPS (1×10^{-5} M) complexed with 1 (5×10^{-5} M) as a function of pH in aqueous 0.1 M NaCl solution at 25 °C.

*NMR spectra of CO adduct of Fe(II)TPPS-***1** *complex*

As previously reported [10], met-hemoCD is reduced to an Fe(II)TPPS-**1** complex (hemoCD) by $Na_2S_2O_4$. HemoCD binds dioxygen (O_2) reversibly in aqueous solution. This is a novel example of Mb or Hb model that works in aqueous solution. The past failure in modeling of Mb function in aqueous solution is mainly due to autoxidation of O_2 adducts by the action of water [14]. Judging from the previous results on the Mb models, it is concluded that the Fe(II) center of hemoCD is very hydrophobic and water is strictly extruded from a cleft formed by the *O*-methylated CD moieties of hemoCD. In order to prove this assumption, we must determine the structure of hemoCD as well as the O_2 adduct of hemoCD (oxy-hemoCD). Since oxy-hemoCD is diamagnetic, NMR study of this compound is theoretically possible. However, gradual autoxidation of oxy-hemoCD takes place leading to difficulty in carrying out this study. Meanwhile, the carbon monoxide (CO) adduct of hemoCD is very stable and hence CO-hemoCD is a suitable compound to deduce the structure of hemoCD and oxy-hemoCD from its spectroscopic measurements.

Figure 7 shows the ^{1}H and ^{13}C NMR spectra of CO-hemoCD. Six singlet signals due to OCH_3 groups at the 2- and 3-positions of the cyclodextrin moieties (vide infra) were observed at 1.5–3.3 ppm. These large high-field shifts of OCH_3 protons should be ascribed to the ring current effects due to the phenyl rings incorporated into the CD cavities of the dimer **1**. In comparison with the ^{13}C NMR spectrum of the intermolecular 1:2

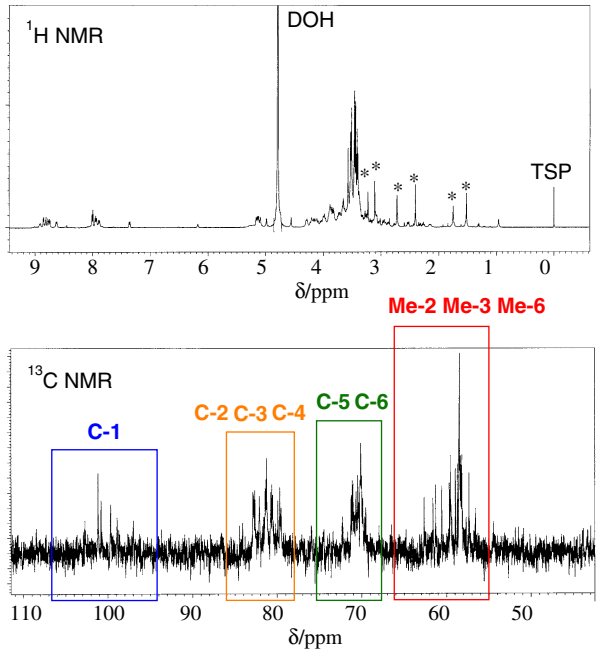

Figure 7. ^{1}H and ^{13}C NMR spectra of CO-hemoCD (5×10^{-3} M) in 0.05 M phosphate buffer at pD 7.0 and 25 °C.

complex of TPPS and TMe-*β*-CD [7b], the ^{13}C NMR signals due to the *O*-methylated *β*-cyclodextrin moieties of the CO-hemoCD are classified into four groups, the (C-1), (C-2, C-3, and C-4), (C-5 and C-6), and (2-, 3-, and 6-OCH_3) groups, as shown in Figure 7. HMQC spectrum (^{1}H-detected multiple quantum coherence spectrum) shown in Figure 8 clearly indicates that the six singlet signals are ascribed to the OCH_3 protons of the dimer **1**. In order to determine the CD cavity side of the OCH_3 groups at higher magnetic fields, HMBC spectrum (^{1}H-detected multiple-bond heteronuclear multiple quantum coherence spectrum) of CO-hemoCD was measured (Figure 9). HMBC spectrum of CO-hemoCD definitely indicates that the six singlet signals are

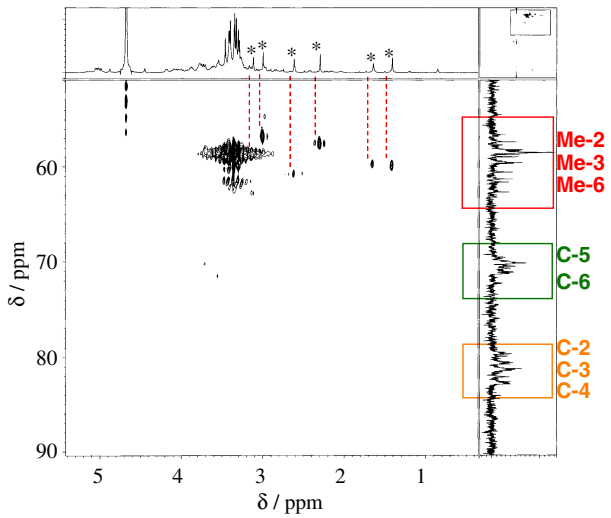

Figure 8. HMQC spectrum of CO-hemoCD (5×10^{-3} M) in 0.05 M phosphate buffer at pD 7.0 and 25 °C.

ascribed to the protons of the OCH_3 groups attached to the 2- and 3-positions of the CD moieties of the dimer **1**. The six-types of OCH_3 groups shifted to the higher magnetic fields strongly suggest that CO-hemoCD takes a completely symmetrical structure. If CO-hemoCD takes an asymmetrical structure, the number of the OCH_3 signals should be more than six because the dimer **1** totally possesses twelve secondary OCH_3 groups. ROESY spectrum (rotating frame nuclear Overhauser and exchange spectrum) of CO-hemoCD (Figure 10) shows the correlation between the six OCH_3 groups and the aromatic rings of TPPS, indicating inclusion of the sulfonatophenyl groups into the cavities of the dimer **1**. All NMR data clearly indicate the formation of CO-hemoCD having a finely symmetrical structure where Fe(II)TPPS is included by the two cyclodextrin moieties

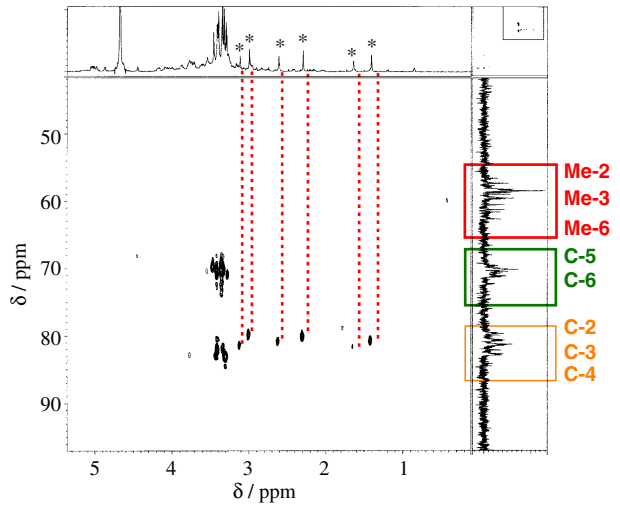

Figure 9. HMBC spectrum of CO-hemoCD (5×10^{-3} M) in 0.05 M phosphate buffer at pD 7.0 and 25 °C.

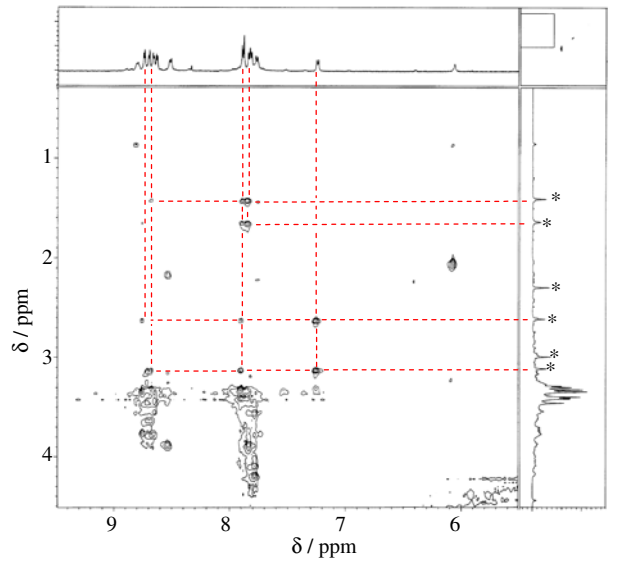

Figure 10. ROESY spectrum of CO-hemoCD (5×10^{-3} M) in 0.05 M phosphate buffer at pD 7.0 and 25 °C.

of the dimer **1** to form the 1:1 complex. In other words, hemoCD and oxy-hemoCD take similar symmetrical structures as shown in Figure 1.

Molecular mechanics calculation of CO-hemoCD

In order to confirm the structure of CO-hemoCD derived from the NMR measurements, molecular mechanics (MM) calculation was carried out by using a BioMedCAChe 6.0 software. In this calculation, the contribution of the solvent, water, was neglected. The result is shown in Figure 11. The energy-minimized structure of CO-hemoCD depends on a structure preformed before calculation. Therefore, the structure in Figure 11 is one of the plausible structures. However, every calculation for various preformed structures indicates the formation of finely symmetrical structure of CO-hemoCD while the degree of covering a porphyrin ring by two CD moieties of the dimer **1** is affected in some extent by the preformed structure. In Figure 11, a CO molecule bound to hemoCD is completely covered by the CD moieties. This structure supports the extremely stable nature of CO-hemoCD. The M value has been used for representing O_2/CO selectivity of Mb, Hb, and their model systems:

$$M = P_{1/2}^{O_2}/P_{1/2}^{CO} \qquad (1)$$

where $P_{1/2}^{O_2}$ and $P_{1/2}^{CO}$ are the O_2 and CO affinities. $P_{1/2}^{L}$ corresponds to the partial pressure at which a half of the Fe(II)porphyrin molecules is coordinated by a ligand such as O_2 or CO. We determined the M value of the present system to be 1.1×10^6 [15]. Such a large M value cannot be explained by a CO–Fe(II) bond strength and stabilization due to hydrogen bonding between bound CO and H_2O. We are assuming covering effect to understand the extremely stable CO adduct of hemoCD. Since back bonding of $d_\pi(\mathrm{Fe}) \rightarrow \pi^*(\mathrm{CO})$ in CO-hemoCD is very weak, the CO–Fe(II) coordination bond is assumed to be weak [15]. Notwithstanding this fact, CO-hemoCD is very stable. This might be ascribed to a cage effect (a covering effect). CO bound to Fe(II) of the dimer **1** is surrounded by the cavities of the CD moieties. Therefore, the CO molecule dissociated from the Fe(II) center cannot move to the aqueous bulk phase leading to rebinding to hemoCD. Similar mechanism might be applied to the naturally occurring systems.

Experimental

Materials

Synthesis of the *O*-methylated *β*-cyclodextrin dimer **1** was described in the previous paper [10]. Fe(III)TPPS and Zn(II)TPPS were prepared according to the procedure described in the previous papers [9, 16]. Water was

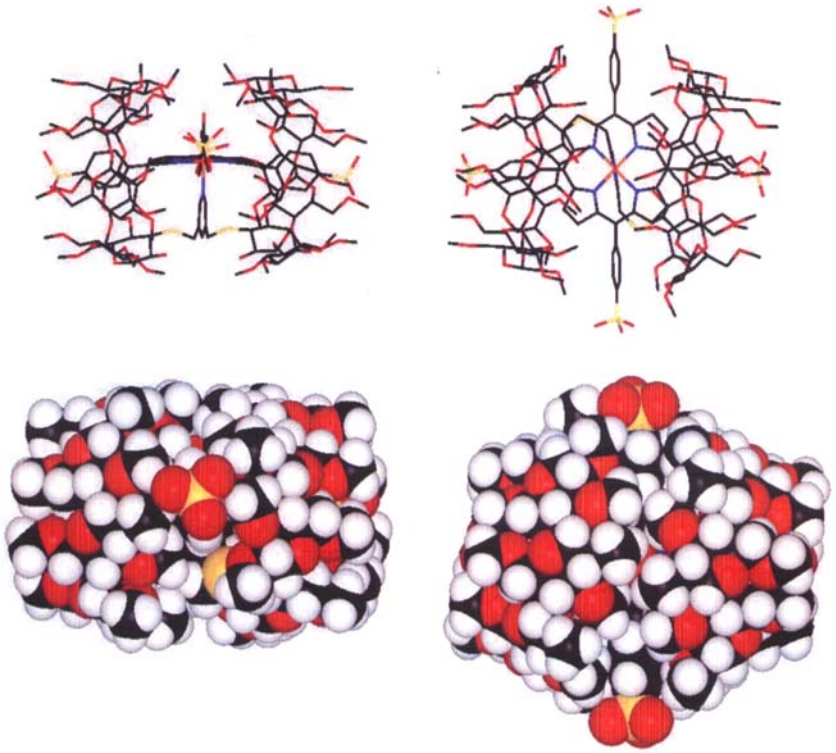

Figure 11. Energy-minimized structures of CO-hemoCD obtained from the MM2 calculations using a BioMedCAChe 6.0. In the stick models (upper), the hydrogen atoms are omitted for clarity. The contribution of the solvent was neglected.

purified using a Millipore Simpak 1. Other chemicals were purchased and used as received.

Measurements

ESI-MS spectrum was recorded on a JEOL JMS-T100CS spectrometer using a negative mode at room temperature. UV–vis absorption spectra were taken using the Shimadzu UV-2100 and UV-2450 spectrophotometers with the thermostatic cell holders. The pH values were measured with a Horiba pH meter M-12. ^{1}H NMR spectra of the Fe(III)TPPS-**1** complex (methemoCD) in D_2O (CEA, 99.9%) were recorded on a JEOL JNM-A400 spectrometer (400 MHz). The solution of CO-hemoCD was prepared by adding two equivalents of $Na_2S_2O_4$ to an aqueous solution of methemoCD (5×10^{-3} M) in 0.05 M phosphate buffer at pH 7.0 under CO atmosphere. ^{1}H (500 MHz), ^{13}C (125 MHz) and 2-D NMR spectra of the CO-hemoCD were recorded on a JEOL JNM-ECA500 spectrometer. The mixing time for the ROESY measurement was 250 ms. Sodium 3-trimethylsilyl [2,2,3,3-$^2H_4$]propionate (TSP, Aldrich) was used as an external standard for NMR measurements.

Acknowledgments

This study was supported by Grants-in-Aid on Scientific Research B (No. 14340224 and 17350074) and on Scientific Research for Priority Area (No. 16041243) from the Ministry of Education, Culture, Sports, Science and Technology, Japan.

References

1. R. Breslow and S.D. Dong: *Chem. Rev.* **98**, 1997 (1998).
2. H. Hirai, N. Toshima, S. Hayashi, and Y. Fujii: *Chem. Lett.* **1983**, 643 (1983).
3. (a) J.S. Manka and D.S. Lawrence: *J. Am. Chem. Soc.* **112**, 2440 (1990); (b) D.L. Dick, T.V.S. Rao, D. Suckumaran, and D.S. Lawrence: *J. Am. Chem. Soc.* **114**, 2664 (1992).
4. (a) S. Mosseri, J.C. Mialocq, B. Perly, and P. Hambright: *J. Phys. Chem.* **95**, 4659 (1991); (b) S. Mosseri and J.C. Mialocq: *Radiat. Phys. Chem.* **37**, 653 (1991); (c) S. Mosseri, J.C. Mialocq, B. Perly, and P. Hambright: *J. Phys. Chem.* **95**, 2196 (1991).
5. J.M. Ribó, J.-A. Farrera, M.L. Valero, and A. Virgili: *Tetrahedron* **51**, 3705 (1995).
6. (a) S.K. Sur and R.G. Bryant: *J. Phys. Chem.* **99**, 4900 (1995); (b) F. Venema, H.F.M. Nelissen, P. Berthault, N. Birlirakis, A.E. Rowan, M.C. Feiters, and R.J.M. Nolte: *Chem. -Eur. J.* **4**, 2237 (1998); (c) J. Mosinger, M. Deumié, K. Lang, P. Kubát, and D.M. Wagnerová: *J. Photochem. Photobiol. A* **130**, 13 (2000).
7. (a) K. Kano, N. Tanaka, H. Minamizono, and Y. Kawakita: *Chem. Lett.* 925 (1996); (b) K. Kano, R. Nishiyabu, T. Asada, and Y. Kuroda: *J. Am. Chem. Soc.* **124**, 9937 (2002).
8. K.J. Kalyanasundaram: *J. Chem. Soc., Faraday Trans 2* **79**, 1365 (1983).
9. K. Kano, H. Kitagishi, S. Tamura, and A. Yamada: *J. Am. Chem. Soc.* **126**, 15202 (2004).
10. K. Kano, H. Kitagishi, M. Kodera, and S. Hirota: *Angew. Chem. Int. Ed.* **44**, 435 (2005).
11. W.R. Sheidt and C.A. Reed: *Chem. Rev.* **81**, 543 (1981).
12. M.A. Ivanca, G.A. Lappin, and W.R. Sheidt: *Inorg. Chem.* **30**, 711 (1991).
13. M. Nappa and J.S. Valentine: *J. Am. Chem. Soc.* **100**, 5075 (1978).
14. (a) D.-L. Jiang and T. Aida: *Chem. Commun.* 1523 (1996); (b) A. Zingg, B. Felber, V. Gramlich, L. Fu, J.P. Collman, and F. Diederich: *Helv. Chem. Acta* **85**, 333 (2002).
15. K. Kano, H. Kitagishi, S. Tanaka, C. Dagallier, M. Kodera, T. Matsuo, T. Hayashi, Y. Hisaeda, and S. Hirota: *Inorg. Chem.* submitted.
16. K. Kano and S. Kobayashi: *Bull. Chem. Soc. Jpn.* **76**, 2027 (2003).